Fisheries Research 252 (2022) 106357

Contents lists available at ScienceDirect

Fisheries Research

journal homepage: www.elsevier.com/locate/fishres

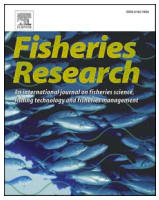

Otolith phenotypic variation as an indicator of stock structure of *Scomberomorus brasiliensis* from the southwestern Atlantic Ocean

Marcelo Soeth [a,b,*], Felippe Alexandre Daros [c], Alberto Teodorico Correia [b,d,e], Nidia Noemi Fabré [f], Reginaldo Medeiros [f], Caroline Vieira Feitosa [g], Oscar de Sousa Duarte [g], Tiago Moraes Lenz [h], Henry Louis Spach [a]

[a] Programa de Pós-Graduação em Sistemas Costeiros e Oceânicos, Universidade Federal do Paraná, P.O 61, 83255-976 Pontal do Paraná, PR, Brazil
[b] Centro Interdisciplinar de Investigação Marinha e Ambiental, Terminal de Cruzeiros do Porto de Leixões, Avenida General Norton de Matos S/N, 4450-208 Matosinhos, Portugal
[c] Universidade Estadual Paulista Julio de Mesquita Filho, UNESP Registro, 11900-000 Registro, SP, Brazil
[d] Faculdade de Ciências da Saúde da Universidade Fernando Pessoa, Rua Carlos Maia 296, 4200-150 Porto, Portugal
[e] Instituto de Ciências Biomédicas Abel Salazar da Universidade do Porto (ICBAS-UP), Rua de Jorge Viterbo Ferreira 228, 4050-313 Porto, Portugal
[f] Laboratory of Ecology, Fish and Fisheries, Institute of Biological and Health Sciences, Federal University of Alagoas, Maceio, Alagoas, Brazil
[g] Laboratório de Dinâmica Populacional e Ecologia de Peixes Marinhos, Instituto de Ciências do Mar, Universidade Federal do Ceará, 60165-081 Fortaleza, Ceará, Brazil
[h] Instituto Federal de Alagoas, Campus Penedo, Alagoas, Brazil

ARTICLE INFO

Handled by B. Morales-Nin

Keywords:
Brazilian coast
Fisheries management
Phenotypic stocks
Thermal gradient
Elliptic Fourier analysis

ABSTRACT

Phenotypic variation of *Scomberomorus brasiliensis* otoliths was evaluated by testing the null hypothesis of a single stock across the southwestern Atlantic Ocean. Otolith sampling of *S. brasiliensis* (n = 396) took place between July and October 2019 at nine locations along the Brazilian coast. The shape of each otolith contour was assessed with elliptic Fourier descriptors (EFDs) and their variation evaluated through multivariate analyses. Fish size-otolith size relationships were used to explore interregional differences in *S. brasiliensis* growth. Cluster analysis based on EFDs separated the sampling locations into tropical (2°S to 20°S) and subtropical (23°S to 27°S) Atlantic regions. The variation of EFDs between these regions was over twice as large as the within region variation. Linear discriminant analysis (LDA) discriminated between regions with 72.85% overall accuracy. Subtropical fish were characterized by the lowest otolith mass at fish size, suggesting great conditions for the growth of *S. brasiliensis* in subtropical waters. Local phenotypic structuring among *S. brasiliensis* population units was less evident (LDA, 29.6% overall accuracy), most likely due to high demographic connectivity on short spatial scales, or even, small environmental heterogeneity to promote discrete phenotypic in *S. brasiliensis* otoliths. Yet, EFDs from distant population units (2°S and 23–27°S) were statistically similar and a likelihood of extensive longshore migration could not be excluded with the herein used approach. These results suggest, however, regional population units appear not regularly mix and fishery managers need to consider such Atlantic regions as functionally distinct management units in a metapopulation perspective.

1. Introduction

The scombrid mackerels fishes are highly adapted to efficiently move long distances, in terms of biology and behavior (Begg et al., 1997; Helfman et al., 2009). Primitive members of the group, such as the *Scomberomorus* genus, tend to live closer to shore (Gold et al., 2010; Zhang et al., 2016). Of the 18 species in the genus *Scomberomorus*, four occur in the Western Atlantic Ocean including *S. cavalla*, *S. maculatus, S. brasiliensis,* and *S. regalis*. The Spanish mackerel, *Scomberomorus brasiliensis* (Collette et al., 1978), inhabit the epipelagic zone mainly between depths of 20 and 60 m along the Atlantic coasts of Central and South America from Belize to southern Brazil (Collette et al., 1978, 2011; Nóbrega and Lessa, 2009). This species can attain a maximum size of at least 125 cm fork length and 6.7 kg (Collette and Nauen, 1983; IGFA, 2021), being exploited by multiple fishing fleets from southern to northern Brazil, which comprises one of the ten most important

* Corresponding author at: Programa de Pós-Graduação em Sistemas Costeiros e Oceânicos, Universidade Federal do Paraná, P.O 61, 83255-976 Pontal do Paraná, PR, Brazil.
E-mail address: marcelosoeth@yahoo.com.br (M. Soeth).

https://doi.org/10.1016/j.fishres.2022.106357
Received 2 September 2021; Received in revised form 24 April 2022; Accepted 27 April 2022
Available online 5 May 2022

commercial fisheries (MPA, 2012). In the past decade, commercial *S. brasiliensis* fisheries landed approximately 10,221 tons per year along the Brazilian coast (MPA, 2012). In tropical waters, *S. brasiliensis* specimens between 2 and 6 years of age represent 86% of the catch composition, whereas individuals older than 11 years of age are less (<5%) frequent (Nóbrega and Lessa, 2009). In this region, sexual maturation occurs at 42 cm FL (around 3–4 years of age), being similar between *S. brasiliensis* males and females (Nóbrega et al., 2004; Nóbrega and Lessa, 2009). In northeast Brazil, this species has been exploited at its maximum sustainable level (Collette et al., 2011), but across southeastern and southern Brazil these levels are unknown. Moreover, there is no specific legislation to ensure the long-term sustainability of *S. brasiliensis* fisheries in Brazil (ICMBio, 2021).

Fisheries management relies on defining spatial units (i.e., stocks units) to set policy frameworks to prevent the overfishing of fish stocks (Secor, 2014). Delineating fish stocks can, however, be challenging, especially for marine organisms which have broad geographical ranges within which biogeographical barriers are unknown, a common issue amongst medium-large sized pelagic fishes such as mackerels (Kritzer and Liu, 2014; Lennox et al., 2019; Pan et al., 2020). Fish stocks are not required to be genetically distinct (Secor, 2014; Punt, 2019). This is because low levels of genetic mixing through one or several past generations are, generally, sufficient to obscure population structure but with minimal demographic consequences (Lowe and Allendorf, 2010; Marengo et al., 2017; Punt, 2019). Therefore, a broad range of techniques based on phenotypic and genetic variation exhibiting distinct spatio-temporal resolutions have been employed for stock delineation, including morphological analyses (Hoff et al., 2020a; Muniz et al., 2021), comparison of life-history traits (Abaunza et al., 2008), otolith shape and elemental analyses (Soeth et al., 2019b; Moura et al., 2020; Correia et al., 2021), and genetic marks (Moreira et al., 2019, 2020). A preliminary study on two distant *S. brasiliensis* populations suggested the absence of spatial significant structure between northern (0°S) and southern (26°S) Brazil using a set of single nucleotide polymorphisms (Siccha-Ramirez et al., 2018). More recently, da Cunha et al. (2020) revealed the existence of a single genetic stock of *S. brasiliensis* on the coast of the southwestern Atlantic using mitochondrial DNA. Despite that, Siccha-Ramirez et al. (2018) found significant differences at five loci between northern and southern Brazil and detected a heterozygote deficit at eight loci for *S. brasiliensis*. The authors argue that the above results could be related to population admixture (Siccha-Ramirez et al., 2018) as would be expected by highly migratory but spatially structured species (Righi et al., 2020). As such, otolith phenotypic attributes may assist in distinguishing between groups of fish that have experienced prolonged separation in heterogeneous environments (Biolé et al., 2019; Soeth et al., 2019b; Muniz et al., 2021).

Otolith shape analysis has been successfully used for fish stock delineation worldwide (Soeth et al., 2019b; Muniz et al., 2021; Schroeder et al., 2021). The shape of otoliths can however be influenced by a variety of factors and not just those associated with fish stock structure (Morales-Nin, 2000; Capoccioni et al., 2011; Vignon, 2012; Teimori et al., 2020). Otolith shape can vary substantially in response to the environments and the habitats that fish use during its lifetime (Campana and Casselman, 1993; Morales-Nin, 2000; Vignon, 2018). The presence of stock-specific otolith shape has been mainly attributed to differences in the rates of somatic and otolith growth, which in turn can be altered by the environment (e.g., temperature, salinity, depth, and diet) experienced by the fish (Mosegaard et al., 1988; Secor and Dean, 1989; Campana and Casselman, 1993; Morales-Nin, 2000; Hüssy, 2008). Moreover, variation in fish metabolic activity can drive differences in otolith size where slow-growing fish commonly exhibit larger otoliths than fast-growing fish of the same size (Mosegaard et al., 1988; Secor and Dean, 1989; Campana and Casselman, 1993). Additionally, the genetic component may influence the otolith shape or act synergistically with the phenotypic-induced otolith characters (Cardinale et al., 2004; Gillanders et al., 2011; Berg et al., 2018). It was therefore considered a priori that (1) variation in the phenotypic of *S. brasiliensis* otoliths from different locations across the Brazilian coast would be indicative of spatial structure; (2) differences in the phenotypic of *S. brasiliensis* otoliths would increase along with water temperature variation; and (3) *S. brasiliensis* otolith mass at fish size variation would be lowest at southern Brazil in response to the greatest growth rates, as recently suggested by Chaves et al. (2021).

In the present work, otolith shape was used to test the null hypothesis of a single phenotypic stock of *S. brasiliensis* across the southwestern Atlantic Ocean. Due to an overall absence of ocean barriers to *S. brasiliensis* along the continental shelf of Brazil, statistical analyses were undertaken firstly comparing all sampling locations; secondly, otolith samples from the tropical Atlantic were compared to otolith samples from the South Brazilian Bight (i.e., subtropical Atlantic) using a nested design to determine scales of significant differences. Finally, fish size-otolith size relationships were used to test the hypothesis that *S. brasiliensis* individuals grew significantly faster in the South Brazilian Bight (SBB) than in tropical oligotrophic waters, which ultimately would support the presence of discrete units in terms of life history.

2. Materials and methods

2.1. Study area and fish sampling

The study area encompassed tropical and subtropical waters of the southwestern Atlantic Ocean, between latitudes 2°S and 27°S (Fig. 1). In this area, two western boundary currents flow along the continental slope: the North Brazil Current (NBC, northward-flowing) and Brazil Current (BC, southward-flowing), both originated from the South Equatorial current (SEC, westward-flowing) branches around 10°S (Silveira et al., 1994; Stramma and England, 1999; Castro et al., 2006). In this long continental shelf, boundary currents have influences on shelf circulation and water mass characteristics (Castro et al., 2006; Palóczy et al., 2016; Combes et al., 2021). The NBC and BC transports two water masses: the warm and oligotrophic Tropical Water (TW) within the mixed layer (0–200 m) (Silveira et al., 1994; Marone et al., 2010) and, at thermocline depths, the South Atlantic Central Water (SACW), which is characterized by relatively low salinities and temperatures (Silveira et al., 1994; Castro and Miranda, 1998; Stramma and England, 1999; Piola et al., 2000). At the inner and medium shelves, coastal water (CW) composition results from the mixing of continental drainage waters, TW, and SACW (Castro et al., 2006; Nogueira and Brandini, 2018).

The physical-chemical properties in the euphotic-mesophotic layers of the tropical-subtropical transition zone (20–23°S) are influenced by coastal upwelling of the cold and nutrient-rich SACW (Cerda and Castro, 2014; Palóczy et al., 2014, 2016). Toward subtropical latitudes, the shelf is subject to bottom intrusions of SACW (Brandini et al., 2014; Castro, 2014), which is considered the most relevant mesoscale physical feature over the SBB (23–28°S) (Nogueira and Brandini, 2018). In addition, wind-driven coastal upwelling off Cape Santa Marta (28.5°S) fertilize the uppers pelagic layers (Vidal et al., 2010; Torquato and Muelbert, 2016). Along with these frontal systems, nearshore estuarine plumes increase regional primary production over the SSB (Brandini et al., 2014; Nogueira and Brandini, 2018).

Samples of *S. brasiliensis* were obtained from local fishers between July and October 2019 at nine locations (Table 1; Fig. 1). A total of 396 *S. brasiliensis* individuals ranging from 41 cm to 65 cm total length (TL, overall mean ± SD= 55.09 ± 4.21 cm TL) were obtained from all locations. The specimens were measured for total length (TL, 1 mm) and sexed by visual inspection of the gonads (Brown-Peterson et al., 2011). Sagittal otoliths were removed using forceps, cleaned of adherent tissues with ultrapure water, and dried with lint-free paper. The otoliths were weighed on an analytical balance (0.0001 g) and stored dry in labeled Eppendorf tubes.

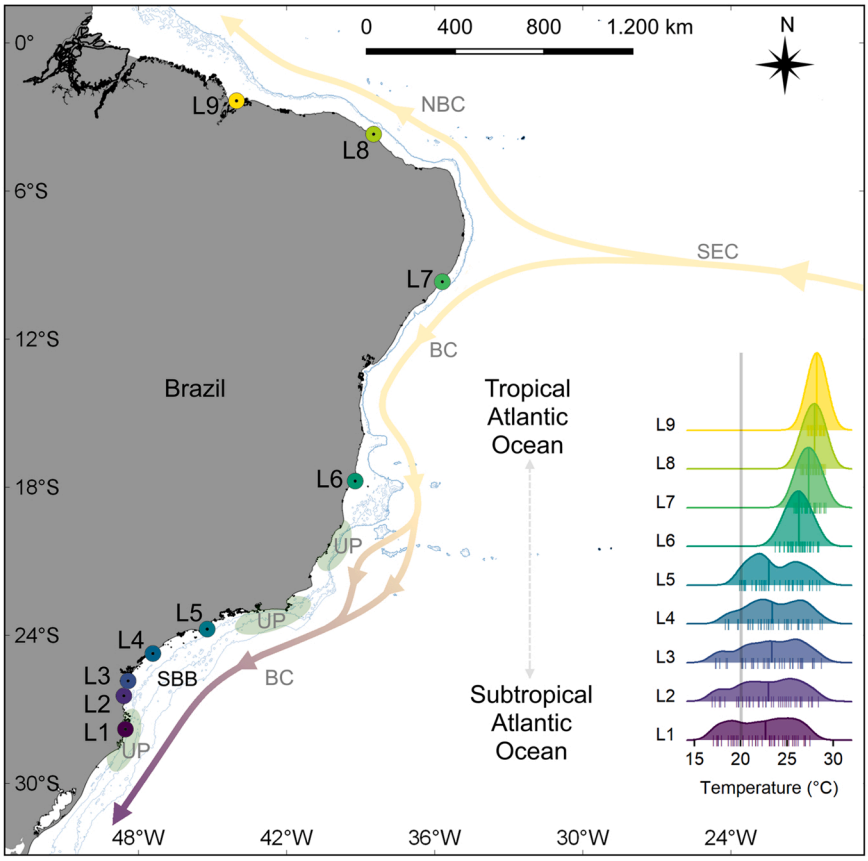

Fig. 1. Brazilian coast showing locations where *Scomberomorus brasiliensis* were obtained from artisanal fishermen. Geostrophic surface currents (upper 100 m) shown are the South Equatorial current (SEC), the North Brazil current (NBC), and the Brazil current (BC) (Stramma and England, 1999). The main coastal upwelling regions (UP) and the South Brazilian Bight (SBB) are also indicated (Castro et al., 2006; Palóczy et al., 2016, 2014). Kernel-smoothed density estimates based on monthly means of sea surface temperature (SST) for each sampling location are shown on the right side of the image. Location codes: Florianópolis (L1), Barra do Sul (L2), Matinhos (L3), Iguape (L4), Ilha Bela (L5), Caravelas (L6), Maceió (L7), Fortaleza (L8), and São Luís (L9).

Table 1
Sampling regions, locations, months in 2019 (from 01 to 12), sample size (n), and mean ± standard deviation of total length (TL) and otolith mass (OM) for *Scomberomorus brasiliensis* from nine locations across the Brazilian coast. Location codes as in Fig. 1.

Region	Location	Months	N	TL (cm)	OM (mg)
Subtropical	L1	07	49	52.64 ± 4.15	19.44 ± 3.20
	L2	08	48	56.55 ± 3.99	22.33 ± 3.87
	L3	07–09	59	53.59 ± 2.70	20.17 ± 2.33
	L4	07	43	59.76 ± 2.60	24.05 ± 2.66
	L5	07	48	56.26 ± 4.25	21.05 ± 2.91
Tropical	L6	09	25	51.02 ± 5.62	20.12 ± 5.26
	L7	10	44	56.14 ± 2.56	24.55 ± 3.84
	L8	09	44	54.89 ± 2.71	25.67 ± 3.50
	L9	10	36	53.36 ± 3.54	20.75 ± 3.41

2.2. Sea surface temperature

To represents the potential environmental heterogeneity experienced by fish groups across the study domain, seawater surface temperature (SST) for each sampling location was obtained from the NASA Soil Moisture Active Passive (SMAP) observatory, produced operationally by Remote Sensing Systems (RSS) (version 4.0 SMAP-SSS level 3 and 70 Km resolution). Monthly means of SST from June 2015 to May 2019 were retrieved from the Physical Oceanography Distributed Active Archive Center (PODAAC, https://podaac.jpl.nasa.gov) and then processed in the SeaWiFS Data Analysis System (SeaDAS Version 7.5.3). The four-year temporal window was defined by estimating the mean age of fish using the inverse function of the von Bertalanffy growth model (Mackay and Moreau, 1990; Daros et al., 2016) considering the growth parameter for *S. brasiliensis* (Nóbrega and Lessa, 2009). Total length was previously transformed to fork length (Chaves et al., 2021).

2.3. Otolith shape analysis

Right sagittal otoliths were systematically placed with the sulcus acusticus facing up and the rostrum pointing left. Two-dimensional digital images of otoliths were captured under a stereomicroscope (×10 magnification) coupled to a camera (Zeiss) with ZEN (blue edition) software. To obtain a good representation of the otolith contour, high-resolution (2560 ×1920) photographs were captured using reflected light against a dark background (Tuset et al., 2008).

Otolith images were read using the shapeR package (Libungan and Pálsson, 2015) written in the programming language R (R Development Core Team, 2021). The shape of each otolith contour was assessed with elliptic Fourier analysis (Kuhl and Giardina, 1982). It decomposes the outline of a two-dimensional object into a series of harmonically related ellipses. Each harmonic yields four coefficients useful as input variables for multivariate statistics (Baylac and Frieß, 2006). The outlines were detected by first transforming the images into grayscale and then converting them to black and white images using a threshold pixel value. Pixel noise around outlines was eliminated using a weighted moving average over three successive coordinate points (Libungan and Pálsson, 2015). The elliptic Fourier descriptors (EFDs) were made invariant with respect to the starting point, scale, rotation, and fish size. Because of the normalization process, the first three descriptors (a1, b1, c1) were omitted (Libungan and Pálsson, 2015). A total of eleven EFDs were excluded due to a significant (ANCOVA, $p < 0.05$) relationship with total length (9 EFDs) or significant interactions with locations (2 EFDs) (Longmore et al., 2010; Libungan and Pálsson, 2015). In the elliptic Fourier analysis, the first six harmonics determine the gross shape of the otolith, such as its circularity and rectangularity. Successively higher-order harmonics measure increasingly finer details in the otolith outline (Kuhl and Giardina, 1982). Therefore, the details of shape reconstruction increase with the number of EDFs along with the

harmonic order used. For *S. brasiliensis* otolith samples, the first 12 harmonics (48–3 = 45 EFDs) adequately described its shape (98.5% accuracy; Supplemental data, Fig. S1), encompassing therefore, the EFDs used through statistical analyses.

2.4. Statistical analysis

All the EFDs were tested for assumptions of univariate normality using the Shapiro–Wilks W test (Shapiro et al., 1968). The hypothesis that the respective distribution is normal was rejected to 19 EFDs (Shapiro-Wilk test, $p < 0.5$) that were excluded from further analyses. For the remaining EFDs (26 variables), the normality assumption was reached (Royston test, $p > 0.05$). Bartlett's test indicated significant homogeneity of variances across groups (Bartlett's K-squared = 7.71, df = 8, p = 0.462).

To identify relevant and homogeneous otolith phenotypic groups, a hierarchical agglomerative, Minimum Variance Clustering (Ward's method), based on the Euclidean distance of the mean values of 26 EFDs was performed (Newman et al., 2009). The agglomerative coefficient (0−1) was used to measure the amount of clustering structure (Kassambara and Mundt, 2020). To test how distinct the *S. brasiliensis* groups are, permutational multivariate analysis of variance (PERMANOVA) and Fisher's Linear Discriminant Analysis (LDA) were performed (Venables and Ripley, 2002). To select reliable and parsimonious variables and to omit variables with the least loss of information (Jenkins and Anderson, 2003; Maugis et al., 2011) a forward-backward stepwise variable selection (stop criterion: improvement less than 0.1%) was performed using the LDA classification function and estimated classification performance by correctness rate (Weihs et al., 2005). To highlight any trends in the stepwise variable selection, a Local Polynomial Regression (LOESS smoother span = 3) was fitted to plots of variable selection (Wickham, 2016). The re-classification of fish individuals was investigated to their true (1) location (nine classes) and (2) groups resulting from the cluster analysis (two classes; tropical and subtropical Atlantic region). The Linear Discriminant (LD) model prediction accuracy was estimated by the percentage of individuals correctly assigned to their actual group using the leave-one-out cross-validation approach (Venables and Ripley, 2002).

Three analytical designs were performed for PERMANOVA. To evaluate differences in otolith shape between sex the design consisted of two factors: location, fixed with 9 levels, and sex, random and nested within locations. There was no significant difference between sexes within locations (PERMANOVA, pseudo-F = 0.811; df=9, 378; p = 0.7798). Thus, males and females' individuals were merged in all analyses. To evaluate the variation among all locations, a one-way PERMANOVA with Location as a fixed factor was performed. A nested design was used to determine scales of significant differences, with two factors: Atlantic region, fixed with 2 levels (subtropical and tropical Atlantic), and location, random and nested within regions. PERMANOVA dissimilarity matrices were based on Euclidean distance measure and Type III (partial) sums of squares were calculated using 9999 permutations of the residuals under a reduced model for nested design and unrestricted permutation of raw data for one-way PERMANOVA. Models found to be statistically significant were followed by permutational pairwise comparisons (pseudo-t statistic) among all pairs of levels (Anderson et al., 2008).

The effect of the Atlantic region (group factor) and fish total length (TL, covariate) on otolith mass (OM, dependent variable) were evaluated with a linear model (LM). The OM and TL were log-transformed (log10) to reach linearity assumption of LM. The Shapiro–Wilks and Levene tests were not significant ($p > 0.05$) showing normality of residuals and homogeneity of variances, respectively. Estimated marginal means of linear trends were used to estimate and compare slope trends (Lenth, 2016). Analysis of Covariance (ANCOVA) was conducted to evaluate significant interactions of the effects of fish TL and Atlantic region on OM.

3. Results

3.1. Sea surface temperature

Monthly means of sea surface temperature (SST) ranged from 16.94 °C to 29.20 °C and showed a clear latitudinal thermal gradient across sampling locations (Fig. 1). Overall mean ± SD (standard deviation) of SST was lowest at L1 (22.37 ± 3.21 °C) and highest at L9 (28.20 ± 0.58 °C). Overall mean of SST northwards of the tropical-subtropical transition zone (L6: 26.21 ± 1.20 °C) was 2.45 °C higher than SST toward subtropical latitudes (L5: 23.76 ± 2.62 °C) (Supplemental data, Table S1).

3.2. Otolith shape variation among locations

The dendrogram resulting from the cluster analysis based on 26 elliptic Fourier descriptors (EFDs), averaged by location, shows two meaningful groupings: *S. brasiliensis* otoliths from tropical (1) and subtropical (2) Atlantic Ocean (Fig. 2a). The agglomerative coefficient (AC = 0.65) indicated a moderate clustering structure. The height of the fusion, provided on the vertical axis, demonstrated that *S. brasiliensis* otolith shape dissimilarity between tropical and subtropical Atlantic (height = 11.09) was twice higher than dissimilarity between the lowest fusions (highest similarities) found to locations within the subtropical Atlantic clusters (Fig. 2a).

To discriminate among *S. brasiliensis* otoliths across locations (Fig. 3a), the variable selection in the model-based discriminant analysis included a subset of nine EFDs (FD4d, FD3d, FD8a, FD8d, FD2c, FD6c, FD10a, FD11a, and FD6b) from low- to high-order harmonics (Supplemental data, Fig. S2). Linear Discriminant axis 1 (LD1) and 2 (LD2) accounted for 80% of data variance, but with high overlap among locations (Fig. 3b). Overall re-classification of individuals based on the LD model was 29.6% only, ranging from 0% (L6) to 61.4% (L8). However, samples were mainly misclassified to close locations (Table 2) suggesting that otolith shapes of neighboring *S. brasiliensis* groups are more like each other. Moreover, scores calculated for LD1 showing negative and positive median for subtropical and tropical locations, respectively, agreed with cluster structure (Fig. 2a and b).

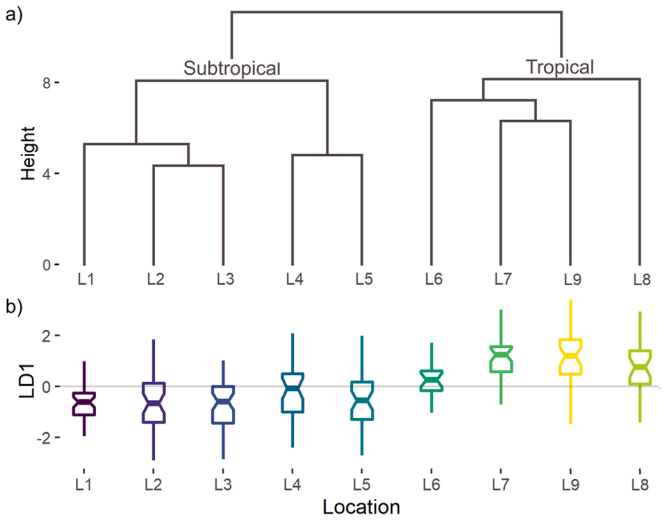

Fig. 2. Dendrogram from Ward hierarchical cluster analysis with Euclidean distance of mean elliptic Fourier descriptors (26 variables) for *S. brasiliensis* otoliths sampled at nine coastal shelf locations of Brazil (a). Scores calculated for Linear discriminant axes 1 based on nine elliptic Fourier descriptors for *S. brasiliensis* otoliths from nine locations (b). Medians are indicated by the bold line, interquartile ranges are indicated by the boxes, and the 95% credible interval is indicated by the whiskers. The notch displays the confidence interval around the median. Location codes as in Fig. 1.

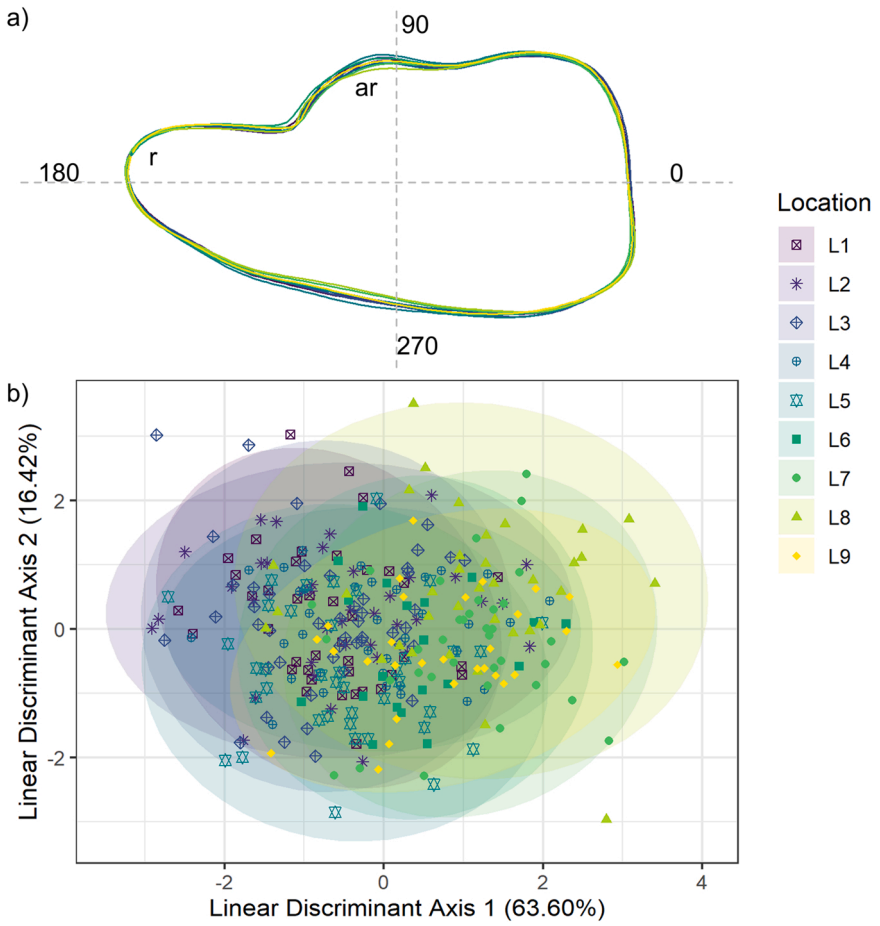

Fig. 3. Mean otolith shape outline based on elliptic Fourier descriptor reconstructions for *S. brasiliensis* (a). Scores calculated for the first two Linear discriminant axes based on nine elliptic Fourier descriptors of *Scomberomurus brasiliensis* otoliths (b). Normal data ellipses (level = 0.95) are drawn around the group centroid. The percentage variance explained by each component is listed on the axes. Image codes: rostrum (r) and anti-rostrum (ar). Locations codes as Fig. 1.

Table 2
Predicted origins of *Scomberomurus brasiliensis* computed from Linear Discriminant Analysis (LDA) based on nine elliptic Fourier descriptors of otolith shape from nine Brazilian coast locations. Location codes as in Fig. 1.

Original group	Predicted group									%overall re-allocation
	L1	L2	L3	L4	L5	L6	L7	L8	L9	
L1	**30.6** (15)	10.2 (5)	26.5 (13)	4.1 (2)	12.2 (6)	4.1 (2)	4.1 (2)	6.1 (3)	2 (1)	29.6
L2	18.8 (9)	**8.3** (4)	29.2 (14)	10.4 (5)	8.3 (4)	2.1 (1)	2.1 (1)	16.7 (8)	4.2 (2)	
L3	15.3 (9)	8.5 (5)	**42.4** (25)	3.4 (2)	15.3 (9)	1.7 (1)	5.1 (3)	6.8 (4)	1.7 (1)	
L4	9.3 (4)	14 (6)	14 (6)	**18.6** (8)	14 (6)	0 (0)	14 (6)	11.6 (5)	4.7 (2)	
L5	6.2 (3)	6.2 (3)	20.8 (10)	4.2 (2)	**43.8** (21)	2.1 (1)	10.4 (5)	6.2 (3)	0 (0)	
L6	8 (2)	8 (2)	16 (4)	8 (2)	20 (5)	**0** (0)	12 (3)	12 (3)	16 (4)	
L7	4.5 (2)	0 (0)	9.1 (4)	0 (0)	11.4 (5)	4.5 (2)	**47.7** (21)	15.9 (7)	6.8 (3)	
L8	6.8 (3)	2.3 (1)	4.5 (2)	6.8 (3)	2.3 (1)	0 (0)	13.6 (6)	**61.4** (27)	2.3 (1)	
L9	11.1 (4)	0 (0)	5.6 (2)	11.1 (4)	8.3 (3)	2.8 (1)	27.8 (10)	19.4 (7)	**13.9** (5)	

%Correct classification in bold and number of otoliths in brackets.

The PERMANOVA combining the subset of nine selected EFDs showed significant differences among *S. brasiliensis* otoliths from coastal shelf locations of Brazil (PERMANOVA, pseudo-$F = 4.229$; df = 8, 395; $p = 0.0001$). Pairwise comparisons (pseudo-*t* test; Table 3) detected that EFDs were similar between all subtropical locations, which were significantly different from L6, L7, and L8. Interestingly, this comparison revealed that *S. brasiliensis* otolith from L9 was similar in shape to L1, L2, and L4 locations (Table 3).

3.3. Otolith shape variation between Atlantic Ocean regions

The shape of *S. brasiliensis* otoliths from subtropical and tropical Atlantic Ocean demonstrated, visually, slight differences at antirostrum (90°) and otolith ventral contour between 180° and 270°. The tropical group was characterized by smoother antirostrum (ar) and narrower rostrum (r) in comparison with the subtropical group (Fig. 5a). Predictions based on the LD model for Atlantic regions included a subset of seven EFDs (FD3d, FD4c, FD2c, FD4d, FD10c, FD9d, and FD7d; Supplemental data, Fig. S2). Re-classification average of individuals to their actual Atlantic Ocean region reached 72.85% (accuracy of 86.6% and 59.1% to subtropical and tropical Atlantic, respectively). With scores calculated for Linear discriminant axes 1 (LD1) for Atlantic Ocean regions there was overlap of the data but not with the confidence interval around the median (i.e., the notch displays; Fig. 4b).

Table 3
Results of permutational pseudo-*t* test of nine elliptic Fourier descriptors for *Scomberomorus brasiliensis* otoliths among all locations. Significant codes: p < 0.0001 '***', p < 0.01 '**', p < 0.05 '*', p < 0.09'`'. Location codes as in Fig. 1.

Locations	pseudo-*t*	Locations	pseudo-*t*	Locations	pseudo-*t*
L1, L2	0.97	L2, L7	2.45**	L4, L8	2.76***
L1, L3	1.26	L2, L8	2.77***	L4, L9	1.59
L1, L4	1.64	L2, L9	1.57	L5, L6	2.63**
L1, L5	1.54	L3, L4	1.11	L5, L7	3.07***
L1, L6	1.87*	L3, L5	1.28	L5, L8	3.71**
L1, L7	2.64**	L3, L6	2.56**	L5, L9	2.07*
L1, L8	2.90***	L3, L7	2.80***	L6, L7	1.53
L1, L9	1.62	L3, L8	3.32***	L6, L8	1.89*
L2, L3	0.58	L3, L9	1.84*	L6, L9	1.15
L2, L4	0.78	L4, L5	1.51	L7, L8	1.55
L2, L5	1.17	L4, L6	2.67**	L7, L9	0.80
L2, L6	2.21*	L4, L7	2.51**	L8, L9	1.36

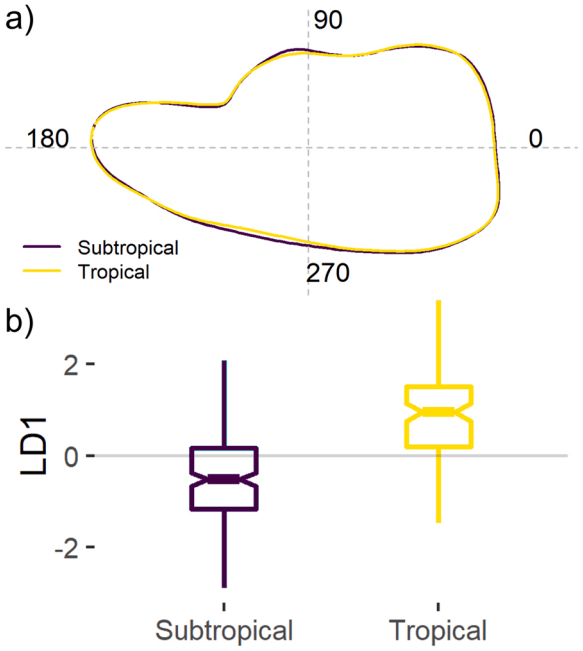

Fig. 4. Mean otolith shape reconstructions (a), and scores calculated for Linear discriminant axes 1 (LD1) based on seven elliptic Fourier descriptors (b) for *Scomberomorus brasiliensis* otoliths from tropical and subtropical Atlantic Ocean. Medians are indicated by the bold line, interquartile ranges are indicated by the boxes, and the 95% credible interval is indicated by the whiskers. The notch displays the confidence interval around the median.

The PERMANOVA combining the subset of seven EFDs from the LD model showed significant differences between *S. brasiliensis* otoliths from subtropical and tropical Atlantic Ocean (PERMANOVA, pseudo-F = 12.931; df = 1, 395; p < 0.0044). Within Atlantic regions, a marginal effect was found at spatial scales of locations (PERMANOVA, pseudo-F = 1.651; df = 7, 395; p < 0.0533). The greatest component of variation (ECV in percentage) estimated from the mean squares occurred at individual fish level (Residual, ECV = 69.06%), followed by Atlantic region (ECV = 22%) and location (8.41%).

The log-transformed OM-TL relationship (Fig. 5) was strongly significant for *S. brasiliensis* (ANCOVA, F = 660.14; df = 1, 391; $p < 0.0001$). The slope was significantly lower (*t-ratio* = −3.59; p < 0.001) for subtropical Atlantic individuals (b = 1.66; CI = 1.49 – 1.83; R^2 = 0.69) in comparison with tropical Atlantic individuals (b = 2.17; CI = 1.95 – 2.39; R^2 = 0.62). That is, *S. brasiliensis* from subtropical Atlantic was characterized by the lowest OM at TL. However, a

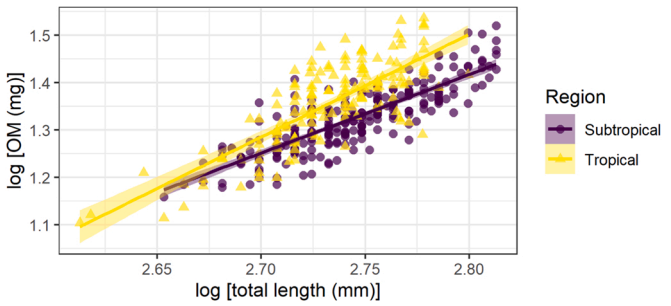

Fig. 5. The log-transformed OM-TL relationship (OM, otolith mass; TL, total length) for *Scomberomorus brasiliensis* from subtropical and tropical Atlantic Ocean. Dots indicate measured values, while the solid line and shading indicate the linear model fitting with 95% confidence intervals, respectively.

significant interaction effect between TL and Atlantic regions indicates that differences in OM between the regions are fish size dependent (ANCOVA, F = 12.90; df = 1, 391; $p < 0.001$), as it can be assessed by visual inspection of the scatter plot and linear model (Fig. 5).

4. Discussion

In the present study, results from a range of statistical analyses were mostly concordant and provide evidence to reject the null hypothesis of a single *S. brasiliensis* fishery stock across the southwestern Atlantic Ocean. In summary, (1) cluster analysis based on EFDs grouped tropical and subtropical locations; (2) the variation of EFDs between these regions was over twice as large as the within region variation; (3) LD model discriminated between Atlantic regions with 72.85% overall accuracy; (4) otolith shapes and OM-TL relationships were significantly different between Atlantic regions. These results suggest individual fish may have experienced distinct environments and that there may be limited mixing between *S. brasiliensis* regional population units (Soeth et al., 2019b; Hoff et al., 2020b; Moura et al., 2020). Despite that, the LD model discriminated among locations with 29.6% overall accuracy only, and otoliths from L9 were statistically similar in shape to L1, L2, and L4, which are over 3550 km apart. Since recent studies have demonstrated an overall absence of genetic structure (SNPs) for *S. brasiliensis* population between northern and southern Brazil (Siccha-Ramirez et al., 2018) and between eastern Venezuela and southern Brazil (mtDNA) (Gold et al., 2010; da Cunha et al., 2020) a hypothesis of exchange among fish individuals from distant population units cannot be excluded with the herein used approach. However, as will be discussed later, a longshore migration between these regions appears unlikely.

Sexual dimorphism in shape was not found for *S. brasiliensis* otoliths and confounding effects on otolith shape (e.g., ontogenetic changes) were minimized to highlight the variation among spatial factors. Yet, the greatest component of variation in shape of *S. brasiliensis* otoliths was found at the individual fish level. In the early life stages of fish, circular larvae otolith shapes undergo several morphological changes as fish transform to juveniles (Brown et al., 2001; Xie et al., 2005; Bounket et al., 2019; Song et al., 2019). After fish reach sexual maturity, otolith shape shows a more constant pattern concerning fish size (Capoccioni et al., 2011; Vignon, 2012; Teimori et al., 2020). Therefore, *S. brasiliensis* individuals were restricted to adults between 410- and 650-mm TL [i.e., approximately 2.8 and 5.5 years old (Nóbrega and Lessa, 2009)], and EFDs were normalized to fish TL to avoid the confounding effect of allometric growth on otolith shape (Libungan and Pálsson, 2015). Several authors, however, have identified fish age used for classification studies is likely to impact classification accuracies using otolith phenotypic as a discriminatory tool (Campana and Casselman, 1993; Mapp et al., 2017). Although it is not always the case (Tracey et al., 2006), age variation at *S. brasiliensis* length could have increased interindividual differences. Additionally, this species can spawn year-round across the

Brazilian coast employing a multiple batch-spawn strategy (Silva et al., 2005; Chaves et al., 2021). This reproduction pattern can lead to an increase in the match or mismatch between the reproduction time and optimal conditions for early life stages growth (Lowerre-Barbieri et al., 1998; Soeth et al., 2019a) that ultimately affect otolith development, and consequently increase interindividual variation of otolith shape (Secor, 1999; Vignon, 2012, 2018).

Scomberomorus brasiliensis individuals from the SBB (i.e., subtropical Atlantic) were characterized by the lowest OM at TL. As many authors have demonstrated that slow-growing fish commonly exhibit larger otoliths than fast-growing fish of the same size (Mosegaard et al., 1988; Secor and Dean, 1989; Casselman, 1990) this finding suggests that *S. brasiliensis* individuals grew significantly faster in subtropical than in tropical waters, as recently suggested by Chaves et al. (2021) using length composition data. The inter-play between SACW intrusions and continental run-off enhances ecosystem productivity from the SBB (Brandini et al., 2018). In this region, a large biomass of sardines, anchovies, and small squids (Matsuura, 1998; Acha et al., 2004; De Freitas and Muelbert, 2004) may give an energetic advantage to *S. brasiliensis* growth and maturation (Menezes, 1970; Barber and Jenkins, 2001). However, TL-OM relationship differences between regions were fish size dependent and, consequently, many hypotheses can be drawn beyond this. For example, a distinct trade-off between somatic growth and reproduction of *S. brasiliensis* because of their earlier maturation in the warm tropical waters (Grande and State, 2004; Folkvord et al., 2014; Chaves et al., 2021). Alternatively, water temperature might change the fish size-otolith size relationship (Pimentel et al., 2014; Martino et al., 2017) and uncouple otolith and somatic growth if temperatures exceed optimal values for fish growth (Mosegaard et al., 1988). Nevertheless, further research is needed to address these hypotheses.

Regional differences in fish growth rates could also have a major contribution to the shape variation of *S. brasiliensis* otoliths across the southwestern Atlantic Ocean (Campana and Casselman, 1993; Fey and Greszkiewicz, 2021; Kikuchi et al., 2021a). Despite the large differences in EFDs between Atlantic regions, *S. brasiliensis* otoliths from L9 were similar in shape to L1, L2, and L4. It is important to highlight that the São Luís coast (L9) is within the Amazonian delta, which encompasses the largest continuous mangrove system in the world (Kjerfve et al., 2002). The continental shelf is wide and under the influence of discharge from many rivers that enhance ecosystem productivity, as observed in the SBB (Smith and Demaster, 1996; Kjerfve et al., 2002; Brandini et al., 2018). Previous studies on *S. brasiliensis* growth across the tropical Atlantic region observed higher growth rates at L9 ($k = 0.29$ year^{-1}; Gonçalves et al., 2003) in comparison with L7 and L8 ($k = 0.15$ year^{-1}; Nóbrega and Lessa, 2009). Since otolith shape is correlated with growth rates (Secor and Dean, 1989; Campana and Casselman, 1993; Hüssy, 2008), such growth trends could have driven convergent otolith shape between L9 and subtropical locations (L1, L2, and L4), where *S. brasiliensis* growth rates appear to be even higher (L3, $k = 0.65$ year^{-1}; Chaves et al., 2021).

Within the SBB, upwelling frontal systems and nearshore estuarine plumes increase environmental heterogeneity (Castro, 2014; Torquato and Muelbert, 2016; Nogueira and Brandini, 2018). These oceanographic features have allowed previous studies using otolith shape analysis to recognize geographically isolated populations units of demersal and pelagic fishes across the SBB, including the Sergeant major *Abudefduf saxatilis* (Adelir-Alves et al., 2019), the Atlantic spadefish *Chaetodipterus faber* (Soeth et al., 2019b), the Bigtooth corvina *Isopisthus parvipinnis* (Hoff et al., 2020b), the Red porgy *Pagrus pagrus* (Kikuchi et al., 2021b), and the Brazilian sardine *Sardinella brasiliensis* (Schroeder et al., 2021). In the present study, by contrast, low shape variation of *S. brasiliensis* otoliths was found between subtropical locations. This finding suggests that *S. brasiliensis* groups moving between subtropical locations yield otoliths that converge to an average shape with no structuring by spatial origin, as found in the white croaker *Micropogonias furnieri* in the same region (Santos et al., 2017).

Fish sampling took place first across the subtropical region between July and early September (winter), which coincides with the highest fisheries landings and pre-spawning period for *S. brasiliensis* at SBB (Chaves et al., 2021; PMAP-BS, 2021). Although there is no catch per unit effort (CPUE) data for this species, interpreting monthly fishery landing of *S. brasiliensis* from SBB (PMAP-BS, 2021) under the hypotheses of a positive relationship between landings biomass and its local abundance, the landing variations within the year should represent, in some degree, seasonal movements of *S. brasiliensis*. Because the caught of this species is uncommon southward L1 (PMAP-BS, 2021), migratory groups should move northward or outward from the shallow waters during the spring and summer months (i.e., spawning season peak; Chaves et al., 2021). Strong seasonality in the *S. brasiliensis* fishery landings also occurs in northern Brazil, where the lowest landings biomass through spring and early summer may reflect movements to spawning grounds (Batista and Fabré, 2001; Nóbrega et al., 2004; Leão et al., 2019). Seasonal migrations between feeding and spawning grounds appear to be a widespread behavior for *Scomberomorus* species worldwide, including *S. queenslandicus* and *S. munroi* from Australian east-coast waters (Begg et al., 1997), for *S. commerson* from eastern Australia (Welsh et al., 2002) and along the Arabian Sea and the Gulf of Oman (Claereboudt et al., 2005), for *S. cavalla* from the Gulf of Mexico and North Atlantic (DeVries et al., 2002), and for *S. niphonius* from East China Sea (Zhang et al., 2016; Pan et al., 2020). In this setting, the lowest reclassification accuracy (0%) recorded for L6 individuals could give some indication of a mixed ground for *S. brasiliensis* stocks. Linear discriminant model reallocated L6 individuals to subtropical (60%) and tropical (40%) locations. Since *S. brasiliensis* post-larvae has been caught across Abrolhos Bank (L6) during the summer (RT25/RRDM, 2019), *S. brasiliensis* from tropical and subtropical stocks may mix at Abrolhos Bank for spawning purposes. If that is the case, this behavior may potentially contribute to gene flow between northern and southern population units. Yet, the phenotype of *S. brasiliensis* otoliths indicated low rates of mixing (<14%) southward of the tropical-subtropical transition zone. In this region, upwelling systems around 20°S and 23°S have been suggested as a biogeographic barrier based on levels of endemicity (Spalding et al., 2007) and division into clades (Santos et al., 2006; Mai et al., 2014; Machado et al., 2017). Although such oceanographic processes may act more as a filter than as a barrier to *S. brasiliensis* (Luiz et al., 2012), the number of successful migrants may decrease along a southward gradient. Seascape differences, trophic dependence, and some degree of philopatry to spawning grounds (Castro et al., 2006; Gold et al., 2010; Chapman et al., 2012) could prevent the dispersion of tropical *S. brasiliensis* individuals southward 23°S.

Results from this study demonstrated moderate to high phenotypic variation for *S. brasiliensis* otoliths across the Brazilian coast during the winter and early spring. Despite the results do not exclude the likelihood of extensive longshore migration for *S. brasiliensis,* distinct region-specific spatial signatures suggest fishery managers need to consider such Atlantic regions as functionally distinct management units. Within the SBB, however, a great overlap regarding the otolith shape may suggest high demographic connectivity on short spatial scales. This finding implies that any local increment in *S. brasiliensis* fishery effort or management would have the potential to affect regional fisheries. In the tropical Atlantic Ocean, appropriate spatial management scales were less evident, and the precautionary management approach should be to consider any such locations as functionally distinct. However, given the nature of otolith shape, additional natural marks (e.g., otolith elemental analysis) and techniques (e.g., mark-recapture) (Soeth et al., 2019b; Moura et al., 2020; McQueen et al., 2021) should be considered to complement this information and to track migration routes during *S. brasiliensis* lifetime.

CRediT authorship contribution statement

Marcelo Soeth: Conceptualization, Formal analysis, Investigation,

Methodology, Writing – original draft, Writing – review & editing. **Felippe Alexandre Daros**: Conceptualization, Resources, Writing – review & editing. **Alberto Teodorico Correia**: Conceptualization, Supervision, Writing – review & editing. **Nidia Noemi Fabré**: Investigation, Writing – review & editing. **Reginaldo Medeiros**: Investigation, Writing – review & editing. **Caroline Vieira Feitosa**: Investigation, Writing – review & editing. **Oscar de Sousa Duarte**: Investigation, Writing – review & editing. **Tiago Moraes Lenz**: Investigation, Writing – review & editing. **Henry Louis Spach**: Conceptualization, Resources, Supervision, Writing – review & editing.

Declaration of Competing Interest

The authors declare that they have no known competing financial interests or personal relationships that could have appeared to influence the work reported in this paper.

Acknowledgements

We thank the Center of Studies of the Sea and the Coastal and Oceanic Systems Post-Graduate Program for logistical support. The first author was funded from a postdoctoral Fellowship provided by the Coordenação de Aperfeiçoamento de Pessoal de Nível Superior from Brazil (CAPES, Process number 88887.357807/2019-00). Correia A.T. is supported by the Portuguese Foundation for Science and Technology (UID/Multi/04423/2019) and by the European Regional Development Fund (PT2020). The authors also wish to thank Ana Claudia Oliveira de Almeida (PGSISCO) and Tunan Thome (UFPR) for their assistance in laboratory work. We thank Nicole Paloshi (PGSISCO) for helpful suggestions regarding SeaWiFS Data Analysis.

Appendix A. Supporting information

Supplementary data associated with this article can be found in the online version at doi:10.1016/j.fishres.2022.106357.

References

Abaunza, P., Gordo, L.S., Santamaría, M.T.G., Iversen, S.A., Murta, A.G., Gallo, E., 2008. Life history parameters as basis for the initial recognition of stock management units in horse mackerel (*Trachurus trachurus*). Fish. Res. 89, 167–180. https://doi.org/10.1016/j.fishres.2007.09.021.

Acha, E.M., Mianzan, H.W., Guerrero, R.A., Favero, M., Bava, J., 2004. Marine fronts at the continental shelves of austral South America: physical and ecological processes. J. Mar. Syst. 44, 83–105. https://doi.org/10.1016/j.jmarsys.2003.09.005.

Adelir-Alves, J., Daros, F.A.L.M., Spach, H.L., Soeth, M., Correia, A.T., 2019. Otoliths as a tool to study reef fish population structure from coastal islands of South Brazil. Mar. Biol. Res. 14, 973–988. https://doi.org/10.1080/17451000.2019.1572194.

Anderson, M.J., Gorley, R.N., Clarke, K.R., 2008. PERMANOVA + For PRIMER: Guide to Software and Statistical Methods. PRIMER-E, Plymouth, UK.

Barber, M.C., Jenkins, G.P., 2001. Differential effects of food and temperature lead to decoupling of short-term otolith and somatic growth rates in juvenile King George whiting. J. Fish Biol. 58, 1320–1330. https://doi.org/10.1006/jfbi.2000.1539.

Batista, V.S., Fabré, N.N., 2001. Temporal and spatial patterns on serra, *Scomberomorus brasiliensis* (Teleostei, Scombridae), catches from the fisheries on the Maranhão coast, Brazil. Braz. J. Biol. 61, 541–546. https://doi.org/10.1590/S1519-69842001000400003.

Baylac, M., Frieß, M., 2006. Fourier descriptors, procrustes superimposition, and data dimensionality: an example of cranial shape analysis in modern human populations. In: Modern Morphometrics in Physical Anthropology. Kluwer Academic Publishers-Plenum Publishers, New York, pp. 145–165. https://doi.org/10.1007/0-387-27614-9_6.

Begg, G.A., Cameron, D.S., Sawynok, W., 1997. Movements and stock structure of school mackerel (*Scomberomorus queenslandicus*) and spotted mackerel (S. munroi) in Australian east-coast waters. Mar. Freshw. Res. 48, 295–301. https://doi.org/10.1071/MF97006.

Berg, F., Almeland, O.W., Skadal, J., Slotte, A., Andersson, L., Folkvord, A., 2018. Genetic factors have a major effect on growth, number of vertebrae and otolith shape in Atlantic herring (*Clupea harengus*). PLoS One 13, e0190995. https://doi.org/10.1371/journal.pone.0190995.

Biolé, F.G., Thompson, G.A., Vargas, C.V., Leisen, M., Barra, F., Volpedo, A.V., Avigliano, E., 2019. Fish stocks of *Urophycis brasiliensis* revealed by otolith fingerprint and shape in the Southwestern Atlantic Ocean. Estuar. Coast. Shelf Sci. 229. https://doi.org/10.1016/j.ecss.2019.106406.

Bounket, B., Gibert, P., Gennotte, V., Argillier, C., Carrel, G., Maire, A., Logez, M., Morat, F., 2019. Otolith shape analysis and daily increment validation during ontogeny of larval and juvenile European chub *Squalius cephalus*. J. Fish Biol. 95, 444–452. https://doi.org/10.1111/jfb.13976.

Brandini, F.P., Tura, P.M., Santos, P.P.G.M., 2018. Ecosystem responses to biogeochemical fronts in the South Brazil Bight. Prog. Oceanogr. 164, 52–62. https://doi.org/10.1016/j.pocean.2018.04.012.

Brandini, F.P., Nogueira, M., Simião, M., Carlos Ugaz Codina, J., Almeida Noernberg, M., 2014. Deep chlorophyll maximum and plankton community response to oceanic bottom intrusions on the continental shelf in the South Brazilian Bight. Cont. Shelf Res. 89, 61–75. https://doi.org/10.1016/j.csr.2013.08.002.

Brown, A.L., Busby, M.S., Mier, K.L., 2001. Walleye pollock *Theragra chalcogramma* during transformation from the larval to juvenile stage: Otolith and osteological development. Mar. Biol. 139, 845–851. https://doi.org/10.1007/s002270100641.

Brown-Peterson, N.J., Wyanski, D.M., Saborido-Rey, F., Macewicz, B.J., Lowerre-Barbieri, S.K., 2011. A standardized terminology for describing reproductive development in fishes. Mar. Coast. Fish. 3, 52–70. https://doi.org/10.1080/19425120.2011.555724.

Campana, S.E., Casselman, J.M., 1993. Stock discrimination using otolith shape analysis. Can. J. Fish. Aquat. Sci. 50, 1062–1083. https://doi.org/10.1139/f93-123.

Capoccioni, F., Costa, C., Aguzzi, J., Menesatti, P., Lombarte, A., Ciccotti, E., 2011. Ontogenetic and environmental effects on otolith shape variability in three Mediterranean European eel (*Anguilla anguilla*, L.) local stocks. J. Exp. Mar. Biol. Ecol. 397, 1–7. https://doi.org/10.1016/j.jembe.2010.11.011.

Cardinale, M., Doering-Arjes, P., Kastowsky, M., Mosegaard, H., 2004. Effects of sex, stock, and environment on the shape of known-age Atlantic cod (*Gadus morhua*) otoliths. Can. J. Fish. Aquat. Sci. 61, 158–167. https://doi.org/10.1139/f03-151.

Casselman, J.M., 1990. Growth and relative size of calcified structures of fish. Trans. Am. Fish. Soc. 119, 673–688. https://doi.org/10.1577/1548-8659(1990)119<0673:GARSOC>2.3.CO;2.

Castro, B., Brandini, F., Pires-Vanin, A., Miranda, L., 2006. Multidisciplinary oceanographic processes on the Western Atlantic continental shelf between 4 N and 34 S. In: Robinson, A.R., Brink, K.H. (Eds.), The Sea, Vol. 14 - The Global Coastal Ocean: Interdisciplinary Regional Studies and Syntheses. Harvard University Press, pp. 259–293.

Castro, B.M., 2014. Summer/winter stratification variability in the central part of the South Brazil Bight. Cont. Shelf Res. 89, 15–23. https://doi.org/10.1016/j.csr.2013.12.002.

Castro, B.M., Miranda, L.B., 1998. Physical oceanography of the western Atlantic continental shelf located between 4°N and 34°S. In: The Sea, vol. 11. ed. John Wiley & Sons, New York.

Cerda, C., Castro, B.M., 2014. Hydrographic climatology of South Brazil Bight shelf waters between São Sebastião (24 S) and Cabo São Tomé (22 S). Cont. Shelf Res. 89, 5–14. https://doi.org/10.1016/j.csr.2013.11.003.

Chapman, B.B., Hulthén, K., Brodersen, J., Nilsson, P.A., Skov, C., Hansson, L.A., Brönmark, C., 2012. Partial migration in fishes: causes and consequences. J. Fish. Biol. 81, 456–478. https://doi.org/10.1111/j.1095-8649.2012.03342.x.

Chaves, P., de, T., da, C., Birnfeld, P.O., Vaz-dos-Santos, A.M., 2021. Population dynamics of *Scomberomorus brasiliensis* from a small-scale fishery off Southern Brazil. Ocean Coast. Res. 69. https://doi.org/10.1590/2675-2824069.20-016pdtdcc.

Claereboudt, M.R., McIlwain, J.L., Al-Oufi, H.S., Ambu-Ali, A.A., 2005. Patterns of reproduction and spawning of the kingfish (*Scomberomorus commerson*, Lacépède) in the coastal waters of the Sultanate of Oman. Fish. Res. 73, 273–282. https://doi.org/10.1016/j.fishres.2005.02.009.

Collette, B.B., Russo, J.L., Zavala-Camin, L.A., 1978. *Scomberomorus brasiliensis*, a new species of Spanish mackerel from the western Atlantic. Fish. Bull. 76, 273–280.

Collette, B., Amorim, A.F., Boustany, A., Carpenter, K.E., de Oliveira Leite Jr., N., Di Natale, A., Fox, W., Fredou, F.L., Graves, J., Viera Hazin, F.H., Juan Jorda, M., Minte Vera, C., Miyabe, N., Nelson, R., Oxenford, H., Teixeira Lessa, R.P., Pires Ferreira Travassos, P.E., 2011. Scomberomorus brasiliensis. The IUCN Red List of Threatened Species 2011:e.T170335A6753567. https://dx.doi.org/10.2305/IUCN.UK.2011–2.RLTS.T170335A6753567.en.

Collette, B.B., Nauen, C.E., 1983. FAO Species Catalogue. Vol. 2. Scombrids of the World: an annotated and illustrated catalogue of tunas, mackerels, bonitos and related species known to date. Food and Agriculture Organization of the United Nations (FAO) Fisheries Synopsis number 125, volume 2.

Combes, V., Matano, R.P., Palma, E., 2021. Circulation and cross-shelf exchanges in the northern shelf region of the southwestern Atlantic: kinematics. J. Geophys. Res. Ocean 1–16. https://doi.org/10.1029/2020jc016959.

Correia, A.T., Moura, A., Triay-Portella, R., Santos, P.T., Pinto, E., Almeida, A.A., Sial, A., Muniz, A.A., 2021. Population structure of the chub mackerel (*Scomber colias*) in the NE Atlantic inferred from otolith elemental and isotopic signatures. Fish. Res. 234, 105785 https://doi.org/10.1016/j.fishres.2020.105785.

da Cunha, D.B., Rodrigues-Filho, L.F.S., de Luna Sales, J.B., Rêgo, P., Queiroz, C., Sampaio, I., Vallinoto, M., 2020. Molecular inferences on *Scomberomorus brasiliensis*, from the western south Atlantic, based on two mitochondrial genes. Front. Mar. Sci. 7, 1–9. https://doi.org/10.3389/fmars.2020.558902.

Daros, F.A., Spach, H.L., Sial, A.N., Correia, A.T., 2016. Otolith fingerprints of the coral reef fish *Stegastes fuscus* in southeast Brazil: a useful tool for population and connectivity studies. Reg. Stud. Mar. Sci. 3, 262–272. https://doi.org/10.1016/j.rsma.2015.11.012.

De Freitas, D.M., Muelbert, J.H., 2004. Ichthyoplankton distribution and abundance off southeastern and southern Brazil. Braz. Arch. Biol. Technol. 47, 601–612. https://doi.org/10.1590/s1516-89132004000400014.

DeVries, D.A., Grimes, C.B., Prager, M.H., 2002. Using otolith shape analysis to distinguish eastern Gulf of Mexico and Atlantic Ocean stocks of king mackerel. Fish. Res. 57, 51–62. https://doi.org/10.1016/S0165-7836(01)00332-0.

Fey, D.P., Greszkiewicz, M., 2021. Effects of temperature on somatic growth, otolith growth, and uncoupling in the otolith to fish size relationship of larval northern pike, *Esox lucius* L. Fish. Res. 236, 105843 https://doi.org/10.1016/j.fishres.2020.105843.

Folkvord, A., Jørgensen, C., Korsbrekke, K., Nash, R.D.M., Nilsen, T., Skjæraasen, J.E., 2014. Trade-offs between growth and reproduction in wild Atlantic cod. Can. J. Fish. Aquat. Sci. 71, 1106–1112. https://doi.org/10.1139/cjfas-2013-0600.

Gillanders, B., Clarke, L.M., Thorrold, S.R., Conover, D.O., 2011. Population differences in otolith chemistry have a genetic basis in *Menidia menidia*. Can. J. Fish. Aquat. Sci. 68, 105–114. https://doi.org/10.1139/F10-147.

Gold, J.R., Jobity, A.M.C., Saillant, E., Renshaw, M.A., 2010. Population structure of carite (*Scomberomorus brasiliensis*) in waters offshore of Trinidad and northern Venezuela. Fish. Res. 103, 30–39. https://doi.org/10.1016/j.fishres.2010.01.009.

Gonçalves, A.P., Dourado, E.C.S., Castro, A.C.L., Tava- Res, R.G.C.F., 2003. Aspectos da dinâmica populacional da serra, *Scomberomorus brasiliensis* (Teleostei, Scombridae), no estado do Maranhão, Brasil. Bol. Labor. Hidrobiol. 16 (1), 37–46.

Grande, R., State, N., 2004. Biologia reprodutiva da serra, *Scomberomorus brasiliensis* (Osteichthyes: Scombridae), em águas costeiras do Rio Grande do Norte. Arq. Ciênc. Mar. 40, 24–30. https://doi.org/10.32360/acmar.v40i1.6139.

Helfman, G.S., Collete, B.B., Facey, D.E., Bowen, B.W., 2009. The Diversity of Fishes: Biology, Evolution, and Ecology, 2nd Edition. Wiley-Blackwell.

Hoff, N.T., Dias, J.F., de Lourdes Zani-Teixeira, M., Soeth, M., Correia, A.T., 2020a. Population structure of the bigtooth corvina *Isopisthus parvipinnis* from the Southwest Atlantic Ocean as determined by whole-body morphology. Reg. Stud. Mar. Sci. 39, 101379 https://doi.org/10.1016/j.rsma.2020.101379.

Hoff, N.T., Dias, J.F., Zani-Teixeira, M., de, L., Correia, A.T., 2020b. Spatio-temporal evaluation of the population structure of the bigtooth corvina *Isopisthus parvipinnis* from Southwest Atlantic Ocean using otolith shape signatures. J. Appl. Ichthyol. 36, 439–450. https://doi.org/10.1111/jai.14044.

Hüssy, K., 2008. Otolith shape in juvenile cod (*Gadus morhua*): Ontogenetic and environmental effects. J. Exp. Mar. Biol. Ecol. 364, 35–41. https://doi.org/10.1016/j.jembe.2008.06.026.

ICMBio, 2021. Instituto Chico Mendes de Conservação da Biodiversidade. ⟨https://www.icmbio.gov.br/⟩. Accessed in 02 September 2021.

IGFA, 2021. World Record Game Fishes. International Game Fish Association, Dania Beach, Florida. ⟨https://igfa.org/igfa-world-records-search⟩. Accessed in 02 September 2021.

Jenkins, L., Anderson, M., 2003. A multivariate statistical approach to reducing the number of variables in data envelopment analysis. Eur. J. Oper. Res. 147, 51–61. https://doi.org/10.1016/S0377-2217(02)00243-6.

Kassambara, A., Mundt, F., 2020. Factoextra: Extract and Visualize the Results of Multivariate Data Analyses. R Package Version 1.0.7.https://CRAN.R-project.org/package=factoextra.

Kikuchi, E., García, S., da Costa, P.A.S., Cardoso, L., Haimovici, M., 2021a. Discrimination of red porgy *Pagrus pagrus* (Sparidae) potential stocks in the Southwestern Atlantic by otolith shape analysis. J. Fish. Biol. 98, 548–556. https://doi.org/10.1111/jfb.14598.

Kikuchi, E., Cardoso, L.G., Canel, D., Timi, J.T., Haimovici, M., 2021b. Using growth rates and otolith shape to identify the population structure of *Umbrina canosai* (Sciaenidae) from the Southwestern Atlantic. Mar. Biol. Res. 0, 1–14. https://doi.org/10.1080/17451000.2021.1938131.

Kjerfve, B., Perillo, G.M., Gardner, L.R., Rine, J.M., Dias, G.T.M., Mochel, F.R., 2002. Morphodynamics of Muddy Environments Along the Atlantic Coasts of North and South America, Muddy Coasts of the World: Processes, Deposits and Functions. Elsevier Science, Amsterdam, pp. 479–532.

Kritzer, J.P., Liu, O.R., 2014. Fishery management strategies for addressing complex spatial structure in marine fish stocks, second ed. ed, Stock Identification Methods. Elsevier. https://doi.org/10.1016/B978–0-12–397003-9.00003–5.

Kuhl, F.P., Giardina, C.R., 1982. Elliptic Fourier features of a closed contour. Comput. Graph. Image Process 18, 236–258. https://doi.org/10.1016/0146-664X(82)90034-X.

Leão, S.A.S., Furtado-Junior, I., Abrunhosa, F.A., Silva, J.A., 2019. Análise histórica de CPUEs padronizadas da serra *Scomberomorus brasiliensis* (pisces: scombridae) desembarcada no estado do Pará - costa Amazônica. Bol. Técnico Cient. CEPNOR 18, 23. https://doi.org/10.32519/tjfas.v18i1.2146.

Lennox, R.J., Paukert, C., Aarestrup, K., Auger-Methe, M., Baumgartner, L., Birnie-Gauvin, K., Bøe, K., Brink, K., Brownscombe, J., Chen, Y., Davidsen, J.G., Eliason, E., Filous, A., Gillanders, B., Helland, I., Horodysky, A., Januchowski-Hartley, S.R., Lowerre-Barbieri, S.K., Lucas, M., Martins, E., Murchie, K., Pompeu, P., Power, M., Raghavan, R., Rahel, F., Secor, D., Thiem, J., Thorstad, E.B., Ueda, H., Whoriskey, F. G., Cooke, S., 2019. 100 pressing questions on the future of global fish migration science, conservation, and policy. Front. Ecol. Evol. 7, 286. https://doi.org/10.3389/FEVO.2019.00286.

Lenth, R.V., 2016. Least-Squares Means: The R Package lsmeans. Journal of Statistical Software 69 (1), 1–33. https://doi.org/10.18637/jss.v069.i01.

Libungan, L.A., Pálsson, S., 2015. ShapeR: an R package to study otolith shape variation among fish populations. PLoS One 10, e0121102. https://doi.org/10.1371/journal.pone.0121102.

Longmore, C., Fogarty, K., Neat, F., Brophy, D., Trueman, C., Milton, A., Mariani, S., 2010. A comparison of otolith microchemistry and otolith shape analysis for the study of spatial variation in a deep-sea teleost, *Coryphaenoides rupestris*. Environ. Biol. Fishes 89, 591–605. https://doi.org/10.1007/s10641-010-9674-1.

Lowe, W.H., Allendorf, F.W., 2010. What can genetics tell us about population connectivity? Mol. Ecol. 19, 3038–3051. https://doi.org/10.1111/j.1365-294X.2010.04688.x.

Lowerre-Barbieri, S.K., Lowerre, J.M., Barbieri, L.R., 1998. Multiple spawning and the dynamics of fish populations: inferences from an individual-based simulation model. Can. J. Fish. Aquat. Sci. 55, 2244–2254. https://doi.org/10.1139/f98-105.

Luiz, O.J., Madin, J.S., Robertson, D.R., Rocha, L. a, Wirtz, P., Floeter, S.R., 2012. Ecological traits influencing range expansion across large oceanic dispersal barriers: insights from tropical Atlantic reef fishes. Proc. R. Soc. B Biol. Sci. 279, 1033–1040. https://doi.org/10.1098/rspb.2011.1525.

Machado, L.F., Damasceno, J., de, S., Bertoncini, Á.A., Tosta, V.C., Farro, A.P.C., Hostim-Silva, M., Oliveira, C., 2017. Population genetic structure and demographic history of the spadefish, *Chaetodipterus faber* (Ephippidae) from Southwestern Atlantic. J. Exp. Mar. Biol. Ecol. 487, 45–52. https://doi.org/10.1016/j.jembe.2016.11.005.

Mackay, D., Moreau, J., 1990. A note on the inverse function of the von Bertalanffy growth function. Fishbyte 1, 23–31.

Mai, A.C.G., Miño, C.I., Marins, L.F.F., Monteiro-Neto, C., Miranda, L., Schwingel, P.R., Lemos, V.M., Gonzalez-Castro, M., Castello, J.P., Vieira, J.P., 2014. Microsatellite variation and genetic structuring in *Mugil liza* (Teleostei: Mugilidae) populations from Argentina and Brazil. Estuar. Coast. Shelf Sci. 149, 80–86. https://doi.org/10.1016/j.ecss.2014.07.013.

Mapp, J., Hunter, E., Van Der Kooij, J., Songer, S., Fisher, M., 2017. Otolith shape and size: the importance of age when determining indices for fish-stock separation. Fish. Res. 190, 43–52. https://doi.org/10.1016/j.fishres.2017.01.017.

Marengo, M., Baudouin, M., Viret, A., Laporte, M., Berrebi, P., Vignon, M., Marchand, B., Durieux, E.D.H., 2017. Combining microsatellite, otolith shape and parasites community analyses as a holistic approach to assess population structure of *Dentex dentex*. J. Sea Res. 128, 1–14. https://doi.org/10.1016/j.seares.2017.07.003.

Marone, E., Knoppers, B., Souza, W.F.L., Silveira, I.C., Godoi, S.S., 2010. The Brazil current: typology and physical-biogeochemical domains. In: Liu, K.-K., Atkinson, L., Quinones, R., Talaue-McManus, L. (Eds.), Carbon and Nutrient Fluxes in Continental Margins: A Global Synthesis. Springer-Verlag, Berlin Heidelberg, pp. 153–170. https://doi.org/10.1007/978-3-540-92735-8.

Martino, J., Doubleday, Z.A., Woodcock, S.H., Gillanders, B.M., 2017. Elevated carbon dioxide and temperature affects otolith development, but not chemistry, in a diadromous fish. J. Exp. Mar. Biol. Ecol. 495, 57–64. https://doi.org/10.1016/j.jembe.2017.06.003.

Matsuura, Y., 1998. Brazilian sardine (*Sardinella brasiliensis*) spawning in the southeast Brazilian Bight over the period 1976-1993. Rev. Bras. Oceanogr. 46, 33–43. https://doi.org/10.1590/s1413-77391998000100003.

Maugis, C., Celeux, G., Martin-Magniette, M.L., 2011. Variable selection in model-based discriminant analysis. J. Multivar. Anal. 102, 1374–1387. https://doi.org/10.1016/j.jmva.2011.05.004.

McQueen, K., Casini, M., Dolk, B., Haase, S., Hemmer-Hansen, J., Hilvarsson, A., Hüssy, K., Mion, M., Mohr, T., Radtke, K., Schade, F.M., Schulz, N., Krumme, U., 2021. Regional and stock-specific differences in contemporary growth of Baltic cod revealed through tag-recapture data. ICES J. Mar. Sci. 77, 2078–2088. https://doi.org/10.1093/ICESJMS/FSAA104.

Menezes, M.F. de, 1970. Alimentação da serra, *Scomberomorus maculatus* (MITCHILL), em águas costeiras do Estado do Ceará. Arq. Ciênc. Mar. 10, 171–176 https://doi.org/http://www.repositorio.ufc.br/handle/riufc/2033.

Morales-Nin, B., 2000. Review of the growth regulation processes of otolith daily increment formation. Fish. Res. 46, 53–67. https://doi.org/10.1016/S0165-7836(00)00133-8.

Moreira, C., Correia, A.T., Vaz-Pires, P., Froufe, E., 2019. Genetic diversity and population structure of the blue jack mackerel *Trachurus picturatus* across its western distribution. J. Fish. Biol. 94, 725–731. https://doi.org/10.1111/jfb.13944.

Moreira, C., Presa, P., Correia, A.T., Vaz-Pires, P., Froufe, E., 2020. Spatio-temporal microsatellite data suggest a multidirectional connectivity pattern in the *Trachurus picturatus* metapopulation from the Northeast Atlantic. Fish. Res. 225, 105499 https://doi.org/10.1016/j.fishres.2020.105499.

Mosegaard, H., Svedäng, H., Taberman, K., 1988. Uncoupling of somatic and otolith growth rates in arctic char (*Salvelinus alpinus*) as an effect of differences in temperature response. Can. J. Fish. Aquat. Sci. 45, 1514–1524. https://doi.org/10.1139/f88-180.

Moura, A., Muniz, A.A., Mullis, E., Wilson, J.M., Vieira, R.P., Almeida, A.A., Pinto, E., Brummer, G.J.A., Gaever, P.V., Gonçalves, J.M.S., Correia, A.T., 2020. Population structure and dynamics of the Atlantic mackerel (*Scomber scombrus*) in the North Atlantic inferred from otolith chemical and shape signatures. Fish. Res. 230, 105621 https://doi.org/10.1016/j.fishres.2020.105621.

MPA, 2012. Boletim de Pesca e Aquicultura 2011. Ministério da Pesca e Aquicultura. http://www.icmbio.gov.br/cepsul/images/stories/ biblioteca/download/estatistica/est_2011_bol_bra.pdf. Accessed in 30 April 2021.

Muniz, A.A., Moura, A., Triay-Portella, R., Moreira, C., Santos, P.T., Correia, A.T., 2021. Population structure of the chub mackerel (*Scomber colias*) in the North-east Atlantic inferred from otolith shape and body morphometrics. Mar. Freshw. Res. 72, 341–352. https://doi.org/10.1071/MF19389.

Newman, S.J., Buckworth, R.C., Mackie, M.C., Lewis, P.D., Wright, I.W., Williamson, P. C., Bastow, T.P., Ovenden, J.R., 2009. Spatial subdivision among assemblages of Spanish mackerel, *Scomberomorus commerson* (Pisces: Scombridae) across northern Australia: implications for fisheries management. Glob. Ecol. Biogeogr. 18, 711–723. https://doi.org/10.1111/j.1466-8238.2009.00475.x.

Nóbrega, M.F. de, Lessa, R.P., 2009. Age and growth of Spanish mackerel (*Scomberomorus brasiliensis*) off the northeastern coast of Brazil. Neotrop. Ichthyol. 7, 667–676. https://doi.org/10.1590/S1679-62252009000400016.

Nóbrega, M.F. de, Frédou, F.L., Lessa, R.P., Hazin, F.V., 2004. Scomberomorus brasiliensis. In: Dinâmica de Populações e Avaliação de Estoques Dos Recursos Pesqueiros Da Região Nordeste v. II, pp. 50–63.

Nogueira, M., Brandini, F.P., 2018. Community structure and spatiotemporal dynamics of the zooplankton in the South Brazilian bight: a review. In: Plankton Ecology of the Southwestern Atlantic. Springer International Publishing, Cham, pp. 149–170. https://doi.org/10.1007/978-3-319-77869-3_8.

Palóczy, A., da Silveira, I.C.A., Castro, B.M., Calado, L., 2014. Coastal upwelling off Cape São Tomé (22°S, Brazil): the supporting role of deep ocean processes. Cont. Shelf Res. 89, 38–50. https://doi.org/10.1016/j.csr.2013.09.005.

Palóczy, A., Brink, K.H., da Silveira, I.C.A., Arruda, W.Z., Martins, R.P., 2016. Pathways and mechanisms of offshore water intrusions on the Espírito Santo Basin shelf (18°S–22°S, Brazil). J. Geophys. Res. Ocean. 121, 5134–5163. https://doi.org/10.1002/2015JC011468.

Pan, X., Ye, Z., Xu, B., Jiang, T., Yang, J., Tian, Y., 2020. Population connectivity in a highly migratory fish, Japanese Spanish mackerel (*Scomberomorus niphonius*), along the Chinese coast, implications from otolith chemistry. Fish. Res. 231, 105690 https://doi.org/10.1016/j.fishres.2020.105690.

Pimentel, M.S., Faleiro, F., Dionisio, G., Repolho, T., Pousao-Ferreira, P., Machado, J., Rosa, R., 2014. Defective skeletogenesis and oversized otoliths in fish early stages in a changing ocean. J. Exp. Biol. 217, 2062–2070. https://doi.org/10.1242/jeb.092635.

Piola, A.R., Campos, E.J.D., Möller, O.O., Charo, M., Martinez, C., 2000. Subtropical shelf front off eastern South America. J. Geophys. Res. Ocean. 105, 6565–6578. https://doi.org/10.1029/1999JC000300.

PMAP-BS, 2021. Programa de Monitoramento da Atividade Pesqueira da Bacia de Santos. Relatório Técnico Semestral (2017–2020). ⟨https://comunicabaciadesantos.petrobras.com.br/programa-ambiental/⟩projeto-de-monitoramento-da-atividade-pesqueira-pmap.html. Accessed in 02 September 2021.

Punt, A.E., 2019. Spatial stock assessment methods: a viewpoint on current issues and assumptions. Fish. Res. 213, 132–143. https://doi.org/10.1016/j.fishres.2019.01.014.

R Development Core Team, 2021. R: a language and environment for statistical computing. R Foundation for statistical computing. Viena, Austria. http://www.R-proje ct.org. Accessed 01 February 2021.

Righi, T., Splendiani, A., Fioravanti, T., Petetta, A., Candelma, M., Gioacchini, G., Gillespie, K., Hanke, A., Carnevali, O., Barucchi, V.C., 2020. Mediterranean swordfish (*Xiphias gladius* Linnaeus, 1758) population structure revealed by microsatellite DNA: Genetic diversity masked by population mixing in shared areas. PeerJ 8. https://doi.org/10.7717/peerj.9518.

RT25/RRDM, 2019. Relatório anual da Rede Rio Doce Mar: Anexo 7 – Ictiofauna e Carcinofauna marinha. http://www.ibama.gov.br/phocadownload/cif/notas-tecnicas/CT-BIO/2019/nt_ctbio_rrdm_rel_anual_rt25_ictiofaunamarinha_19.pdf. Accessed in 02 September 2021.

Santos, R., da, S., Azevedo, M.C.C., de, Albuquerque, C.Q., de, Araújo, F.G., 2017. Different sagitta otolith morphotypes for the whitemouth croaker *Micropogonias furnieri* in the Southwestern Atlantic coast. Fish. Res. 195, 222–229. https://doi.org/10.1016/j.fishres.2017.07.027.

Santos, S., Hrbek, T., Farias, I.P., Schneider, H., Sampaio, I., 2006. Population genetic structuring of the king weakfish, *Macrodon ancylodon* (Sciaenidae), in Atlantic coastal waters of South America: deep genetic divergence without morphological change. Mol. Ecol. 15, 4361–4373. https://doi.org/10.1111/j.1365-294X.2006.03108.x.

Schroeder, R., Schwingel, P.R., Correia, A.T., 2021. Population structure of the Brazilian sardine (*Sardinella brasiliensis*) in the Southwest Atlantic inferred from body morphology and otolith shape signatures. Hydrobiologia 7. https://doi.org/10.1007/s10750-021-04730-7.

Secor, D.H., 1999. Specifying divergent migrations in the concept of stock: the contingent hypothesis. Fish. Res. 43, 13–34. https://doi.org/10.1016/S0165-7836(99)00064-8.

Secor, D.H., 2014. The unit stock concept: bounded fish and fisheries. In: Cadrin, S.X., Kerr, L.A., Mariani, S. (Eds.), Stock Identification Methods: Applications in Fishery Science, second ed. Elsevier, pp. 7–28. https://doi.org/10.1016/B978-0-12-397003-9.00002-3.

Secor, D.H., Dean, J.M., 1989. Somatic growth effects on the otolith–fish size relationship in young pond-reared striped bass, *Morone saxatilis*. Can. J. Fish. Aquat. Sci. 46 (1), 113–121. https://doi.org/10.1139/f89-015.

Shapiro, S., Wilk, M., Chen, H., 1968. A Comparative Study of Various Tests for Normality. J. Am. Stat. Assoc. 63, 1343–1372. https://doi.org/10.1080/01621459.1968.10480932.

Siccha-Ramirez, Z.R., Maroso, F., Pardo, B.G., Fernández, C., Martínez, P., Oliveira, C., 2018. SNP identification and validation on genomic DNA for studying genetic diversity in *Thunnus albacares* and *Scomberomorus brasiliensis* by combining RADseq and long read high throughput sequencing. Fish. Res. 198, 189–194. https://doi.org/10.1016/j.fishres.2017.09.002.

Silva, G.C.Da, Castro, A.C.L., De, Gubiani, É.A., 2005. Population structure and reproductive index of *Scomberomorus brasiliensis* Collette, Russo & Zavala-Camin, 1978 (Perciformes: Scombridae) in western coast of Maranhão. Acta Sci. Biol. Sci. 27, 383–389.

Silveira, I.C.A., da, Miranda, L.B., Brown, W.S., 1994. On the origins of the North Brazil Current. J. Geophys. Res. 99, 501–512. https://doi.org/10.1029/94JC01776.

Smith, W.O., Demaster, D.J., 1996. Phytoplankton biomass and pro- ductivity in the Amazon River plume: correlation with seasonal river discharge. Cont. Shelf Res. 16 (3), 291–319. https://doi.org/10.1016/0278-4343(95)00007-N.

Soeth, M., Fávaro, L.F., Spach, H.L., Daros, F.A., Woltrich, A.E., Correia, A.T., 2019a. Age, growth, and reproductive biology of the Atlantic spadefish *Chaetodipterus faber* in southern Brazil. Ichthyol. Res. 66, 140–154. https://doi.org/10.1007/s10228-018-0663-2.

Soeth, M., Spach, H.L., Daros, F.A., Adelir-Alves, J., de Almeida, A.C.O., Correia, A.T., 2019b. Stock structure of Atlantic spadefish *Chaetodipterus faber* from Southwest Atlantic Ocean inferred from otolith elemental and shape signatures. Fish. Res. 211, 81–90. https://doi.org/10.1016/j.fishres.2018.11.003.

Song, Y., Cheng, F., Zhao, S., Xie, S., 2019. Ontogenetic development and otolith microstructure in the larval and juvenile stages of mandarin fish *Siniperca chuatsi*. Ichthyol. Res. 66, 57–66. https://doi.org/10.1007/s10228-018-0648-1.

Spalding, M.D., Fox, H.E., Allen, G.R., Davidson, N., Ferdaña, Z.A., Finlayson, M., Halpern, B.S., Jorge, M.A., Lombana, A., Lourie, S.A., Martin, K.D., McManus, E., Molnar, J., Recchia, C.A., Robertson, J., 2007. Marine ecoregions of the world: a bioregionalization of coastal and shelf areas. Bioscience 57, 573–583. https://doi.org/10.1641/B570707.

Stramma, L., England, M., 1999. On the water masses and mean circulation of the South Atlantic Ocean. J. Geophys. Res. Ocean. 104, 20863–20883. https://doi.org/10.1029/1999JC900139.

Teimori, A., Motamedi, M., Zeinali, F., 2020. Intrapopulation variation of otolith associated with ontogeny and morphological dimorphism in Hormuz tooth-carp *Aphanius hormuzensis* (Teleostei: Aphaniidae). Acta Zool. 1–15. https://doi.org/10.1111/azo.12332.

Torquato, F., Muelbert, J.H., 2016. Spatial distribution of eggs and larvae of *Engraulis anchoita* (Hubbs & Amp; Marini, 1935) in the southern brazilian shelf. Brazilian. J. Aquat. Sci. Technol. 19. https://doi.org/10.14210/bjast.v19n3.4653.

Tracey, S.R., Lyle, J.M., Duhamel, G., 2006. Application of elliptical Fourier analysis of otolith form as a tool for stock identification. Fish. Res. 77, 138–147. https://doi.org/10.1016/j.fishres.2005.10.013.

Tuset, V.M., Lombarte, A., Assis, C.A., 2008. Otolith atlas for the western Mediterranean, north and central eastern Atlantic. Sci. Mar. 72, 7–198. https://doi.org/10.3989/scimar.2008.72s17.

Venables, W.N., Ripley, B.D., 2002. Modern Applied Statistics with S, Fourth Edition. Springer, New York. ISBN 0-387-95457-0.

Vidal, E.A.G., Haimovici, M., Hackbart, V.C.S., 2010. Distribution of paralarvae and small juvenile cephalopods in relation to primary production in an upwelling area off southern Brazil. ICES J. Mar. Sci. 67, 1346–1352. https://doi.org/10.1093/icesjms/fsq080.

Vignon, M., 2012. Ontogenetic trajectories of otolith shape during shift in habitat use: interaction between otolith growth and environment. J. Exp. Mar. Biol. Ecol. 420–421, 26–32. https://doi.org/10.1016/j.jembe.2012.03.021.

Vignon, M., 2018. Short-term stress for long-lasting otolith morphology — brief embryological stress disturbance can reorient otolith ontogenetic trajectory. Can. J. Fish. Aquat. Sci. 75, 1713–1722. https://doi.org/10.1139/cjfas-2017-0110.

Weihs, C., Ligges, U., Luebke, K., Raabe, N., 2005. klaR Analyzing German Business Cycles. In: Baier, D., Decker, R., Schmidt-Thieme, L. (Eds.), Data Analysis and Decision Support. Springer-Verlag, Berlin, pp. 335–343.

Welsh, D.J., Hoyle, S.D., McPherson, G.R., Gribble, N.A., 2002. Preliminary assessment of the Queensland east coast spanish mackerel fishery. In: Information Series, QI02110,. Queensland Gov- ernment, Department of Primary Industries, Cairs.

Wickham, H., 2016. ggplot2: Elegant Graphics for Data Analysis. Springer-Verlag. https://ggplot2.tidyverse.org/. Accessed 01 February 2021.

Xie, S., Watanabe, Y., Saruwatari, T., Masuda, R., Yamashita, Y., Sassa, C., Konishi, Y., 2005. Growth and morphological development of sagittal otoliths of larval and early juvenile *Trachurus japonicus*. J. Fish. Biol. 66, 1704–1719. https://doi.org/10.1111/j.0022-1112.2005.00717.x.

Zhang, C., Ye, Z., Li, Z., Wan, R., Ren, Y., Dou, S., 2016. Population structure of Japanese Spanish mackerel *Scomberomorus niphonius* in the Bohai Sea, the Yellow Sea and the East China Sea: evidence from random forests based on otolith features. Fish. Sci. 82, 251–256. https://doi.org/10.1007/s12562-016-0968-x.